Carrier diffusion in $Cd_{1-x}Mn_xTe$

C. Moussu, I. Zaquine, and A. Maruani
Ecole Nationale Supérieure des Télécommunications, Département Traitement du Signal et des Images, 46 rue Barrault, 75634 Paris Cédex 13, France

R. Frey
Ecole Nationale Supérieure des Télécommunications, Département Traitement du Signal et des Images, 46 rue Barrault, 75634 Paris Cédex 13, France
and Laboratoire d'Optique Quantique du Centre National de la Recherche Scientifique, Ecole Polytechnique, 91128 Palaiseau Cédex, France
(Received 23 February 1998)

Carrier diffusion and electron-hole recombination are shown to be considerably slowed down in $Cd_{1-x}Mn_xTe$ semimagnetic semiconductors due to the efficient trapping of electrons on manganese sites. The theoretical interpretation is based on population dynamics, charge continuity equations, and Poisson's law. A simple analytical solution of this complicated system of equations is in very good agreement with the numerical one for a large range of durations of the write pulses (from 100 ps to 1 μs). Both calculations predict a reduction of electron mobility by a factor of 6000. These theoretical predictions are confirmed by the results of an experimental study performed by using the simple grating technique: We observe the temporal evolution of the diffracted signal when a continuous read beam is used to read gratings of different wavelengths encoded in the material by interfering write laser pulses. An effective ambipolar mobility of 0.54 $cm^2/V\,s$ is measured, which provides a value of 3400 $cm^2/V\,s$ for the intrinsic mobility in $Cd_{0.7}Mn_{0.3}Te$. This low ambipolar mobility could make this efficient material potentially interesting for parallel optical processing in the microsecond range. [S0163-1829(98)03436-5]

I. INTRODUCTION

Carriers can be created in semiconductors either electronically through injection in diodes or optically through optical absorption. The mobility of these carriers strongly influences the properties of the medium. For example, a high mobility is required to speed up electronic devices while a low extrinsic mobility is necessary for optical recording of long-lived diffraction gratings in semiconductor media. Indeed, the intrinsic mobility corresponding to a pure material can be lowered by introduction of traps, leading to the so-called extrinsic mobility. In the case of pure II-VI semiconductors such as CdTe, electron mobilities of the order of 1100 $cm^2/V\,s$ can be obtained.[1] In the case of $Cd_{1-x}Mn_xTe$ semimagnetic semiconductors, it was recently shown that recombination is drastically reduced by trapping of electrons on the manganese sites,[2] especially in very pure samples. This effect is expected to lead to a lowering of electron mobility, which strongly modifies carrier diffusion.

In this paper we show, both theoretically and experimentally, that diffusion of free carriers photogenerated in $Cd_{1-x}Mn_xTe$ semimagnetic semiconductors (SMSC's) is drastically reduced owing to efficient trapping of electrons, most probably on manganese sites. This mechanism is observed through the grating technique,[3] where free carrier (electron and hole) gratings are photogenerated through absorption of interfering laser beams in the $Cd_{1-x}Mn_xTe$ sample. Due to the very fast ($\tau<1$ ps) trapping of electrons on the manganese sites, a grating of quasifixed negative charges is created and the diffusion of the associated hole grating is much reduced. The hole density modulation gives rise to a long-lived refractive index grating. Moreover, due to hole diffusion, the modulation amplitudes of positive and negative charges are slightly different, hence a space charge field that produces a photorefractive grating in this electro-optic material. Measurement of the time evolution of the diffraction efficiency of these photogenerated gratings allows the study of carrier diffusion in this material.

II. THEORY

A. Description of the model

The model used to determine theoretically the free hole and photorefractive contributions to the refractive index grating is extrapolated from that used to explain the long-lived fluorescence[4] and photoinduced Faraday rotation[5] previously observed in $Cd_{1-x}Mn_xTe$ SMSC's. This model is depicted in Fig. 1. It contains four levels: the conduction and valence bands (with state densities C and H, respectively), a trap level (with state density P), and a recombination level (with state density R) from which radiative recombination occurs with free holes. These two last levels are located at $\Delta_P = 13$ meV and $\Delta_R = 210$ meV below the conduction band.[2] Population transfers between the conduction band, the trap level, and the recombination center level are evaluated by using the relaxation constants (K_R, K_P, and K_H for the $C \rightarrow R$, $C \rightarrow P$, and $R \rightarrow H$ transitions) and the thermally activated relaxation constants ($K'_R = K_R \exp[-(\Delta_R/k_BT)]$ and $K'_P = K_P \exp[-(\Delta_P/k_BT)]$) with k_B the Boltzmann constant and T the sample temperature. The system is described by population rate equations for the fixed trap and recombination level densities (p and r, respectively), continuity equa-

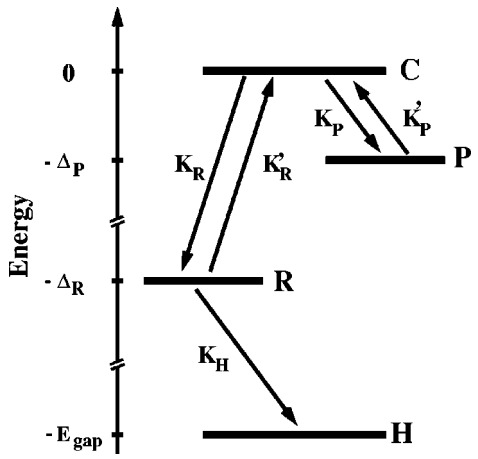

FIG. 1. Scheme of the relaxation model for optically induced carriers.

tions for electron and hole densities (c and h, respectively), and Poisson's law for the space charge field $\underline{E}$. The following set of space- and time-dependent differential equations is then obtained:

$$\frac{\partial c}{\partial t}=\mu_e\underline{\nabla}\cdot(c\underline{E})+\frac{\mu_e k_B T}{e}\Delta c+sI-K_P c(P-p)+K'_P p(C-c)-K_R c(R-r)+K'_R r(C-c), \quad (1)$$

$$\frac{\partial r}{\partial t}=K_R c(R-r)-K'_R r(C-c)-K_H rh, \quad (2)$$

$$\frac{\partial p}{\partial t}=K_P c(P-p)-K'_P p(C-c), \quad (3)$$

$$\frac{\partial h}{\partial t}=-\mu_h\underline{\nabla}\cdot(h\underline{E})+\frac{\mu_h k_B T}{e}\Delta h-K_H rh+sI, \quad (4)$$

$$\underline{\nabla}\cdot\underline{E}=-\frac{e}{\varepsilon_0\varepsilon_s}[c+p+r-h]. \quad (5)$$

In Eqs. (1)–(5), e is the modulus of the charge of electron, ε_S is the static dielectric constant, μ_e and μ_h are the intrinsic electron and hole mobilities, respectively, and sI is the excitation rate expressed in (photons/s)/cm^3 with $I=I(\vec{r},t)$ the local intensity.

B. Numerical solution

The problem is solved with a light grating of wave vector $\underline{K}$ along the x axis $[I(\vec{r},t)=I_0(t)(1+m\cos Kx)]$ with a low contrast ($m\ll 1$) in the case of no externally applied electric field. Setting $b=b_0+[(\Delta b/2)\exp(iKx)+\text{c.c.}]$ with $b=p,r,c,h,E$, we get two sets of coupled, time-dependent, differential equations

$$\frac{dc_0}{dt}=-K_P c_0(P-p_0)+K'_P p_0(C-c_0)-K_R c_0(R-r_0)+K'_R r_0(C-c_0)+sI_0, \quad (6)$$

$$\frac{dr_0}{dt}=K_R c_0(R-r_0)-K'_R r_0(C-c_0)-K_H r_0 h_0, \quad (7)$$

$$\frac{dp_0}{dt}=K_P c_0(P-p_0)-K'_P p_0(C-c_0), \quad (8)$$

$$\frac{dh_0}{dt}=-K_H r_0 h_0+sI_0, \quad (9)$$

$$E_0=0 \quad (10)$$

for the mean densities c_0, r_0, p_0, h_0, and E_0 and

$$\frac{d\Delta c}{dt}=K'_R[\Delta r(C-c_0)-r_0\Delta c]-K_R[\Delta c(R-r_0)-c_0\Delta r]+K'_P[\Delta p(C-c_0)-p_0\Delta c]-K_P[\Delta c(P-p_0)-c_0\Delta p]-\frac{\Delta c}{\tau_{D_e}}-\frac{\Delta p+\Delta r+\Delta c-\Delta h}{\tau_{di_e}}+msI_0, \quad (11)$$

$$\frac{d\Delta r}{dt}=K_R[\Delta c(R-r_0)-c_0\Delta r]-K'_R[\Delta r(C-c_0)-r_0\Delta c]-K_H[r_0\Delta h+h_0\Delta r], \quad (12)$$

$$\frac{d\Delta p}{dt}=K_P[\Delta c(P-p_0)-c_0\Delta p]-K'_P[\Delta p(C-c_0)-p_0\Delta c], \quad (13)$$

$$\frac{d\Delta h}{dt}=-K_H[r_0\Delta h+h_0\Delta r]-\frac{\Delta h}{\tau_{D_h}}+\frac{\Delta p+\Delta r+\Delta c-\Delta h}{\tau_{di_h}}+msI_0, \quad (14)$$

$$\Delta E=i\frac{e}{\varepsilon_0\varepsilon_s K}[\Delta c+\Delta p+\Delta r-\Delta h] \quad (15)$$

for the modulation amplitudes Δc, Δr, Δp, Δh, and ΔE. In Eqs. (11)–(15), $\tau_{D_e}=e/\mu_e k_B T K^2$ and $\tau_{D_h}=e/\mu_h k_B T K^2$ are the characteristic diffusion lifetimes of electrons and holes, respectively, and $\tau_{di_e}=\varepsilon_0\varepsilon_S/e\mu_e c_0$ and $\tau_{di_h}=\varepsilon_0\varepsilon_S/e\mu_h h_0$ are the dielectric time constants for electrons and holes, respectively.

These equations were solved numerically for a top hat intensity profile of width $\Delta t=10$ ps to a few μs using the system constants[2] $P=1.2\times10^{22}$ cm^{-3}, $R=1.2\times10^{16}$ cm^{-3}, $C=1.6\times10^{18}$ cm^{-3}, $K_R=5\times10^{-4}$ s^{-1} cm^{-3}, $K_P=5\times10^{-10}$ s^{-1} cm^{-3}, $K_H=2.6\times10^{-9}$ s^{-1} cm^{-3}, and $T=300$ K. Whatever pulse duration was used, the density of photogenerated electron-hole pairs was constant ($sI_0\Delta t=10^{16}$ cm^{-3}). Results are presented in Secs. II D and II E.

C. Analytical solution

A simple analytical solution of Eqs. (1)–(5) was also performed under the assumptions of low excitation rate ($C\gg c$, $R\gg r$, and $P\gg p$) and low space charge density (D

$=p+r+c-h \ll h$). We therefore obtain, when assuming a low recombination rate for holes ($K_H rt \ll 1$),

$$\frac{\partial p}{\partial t} = K_P P c - K'_P C p, \tag{16}$$

$$\frac{\partial r}{\partial t} = K_R R c - K'_R C r, \tag{17}$$

$$\frac{\partial h}{\partial t} = \frac{\mu_e k_B T}{e}\left(\frac{\partial^2 c}{\partial x^2} + \frac{c}{h}\frac{\partial^2 h}{\partial x^2}\right) + \mu_e E\left(\frac{\partial c}{\partial x} - \frac{c}{h}\frac{\partial h}{\partial x}\right) + sI, \tag{18}$$

$$\frac{\partial D}{\partial t} = \mu_h E \frac{\partial h}{\partial x} - \frac{\mu_h e}{\varepsilon_0 \varepsilon_S} hD - \frac{\mu_h k_B T}{e}\frac{\partial^2 h}{\partial x^2}, \tag{19}$$

$$\frac{\partial E}{\partial x} = -\frac{e}{\varepsilon_0 \varepsilon_S} D. \tag{20}$$

Equations (18) and (19) are obtained through linear combinations of Eqs. (1)–(4), replacing $\underline{\nabla} \cdot \underline{E}$ by its expression in Eq. (5). Equation (18) comes from the calculation of $\mu_e c(\partial h/\partial t) + \mu_h h[\partial(p+r+c)/\partial t]$, which becomes $\mu_h h(\partial h/\partial t)$ if $p+r+c \approx h$ and $\mu_e c \ll \mu_h h$. Equation (19) is simply Eq. (1) plus Eq. (2) plus Eq. (3) minus Eq. (4), assuming $\mu_e c \ll \mu_h h, \mu_e(\partial c/\partial x) \ll \mu_h(\partial h/\partial x)$ and $\mu_e(\partial^2 c/\partial^2 x) \ll \mu_h(\partial^2 h/\partial^2 x)$, which is generally true even with $\mu_e = 5700$ cm^2/V s and $\mu_h = 40$ cm^2/V s.[6]

Resolution of Eqs. (16)–(20) at zeroth order with respect to m gives the following expressions for the mean densities during the top hat pulse:

$$c_0 = \frac{sI_0}{K_P P}\left[1 + K'_P C t - \frac{K_R R}{K_P P + K_R R}\exp\left(-\frac{t}{\tau_2}\right) - \frac{K_P P}{K_P P + K_R R}\exp\left(-\frac{t}{\tau_1}\right)\right], \tag{21}$$

$$r_0 = \frac{sI_0}{K'_R C}\frac{K_R R}{K_P P}\left[1 + K'_P C t - \exp\left(-\frac{t}{\tau_2}\right)\right], \tag{22}$$

$$p_0 = \frac{sI_0}{K'_R C}\left[K'_R\, C t - 1 + \exp\left(-\frac{t}{\tau_2}\right)\right], \tag{23}$$

$$h_0 = sI_0 t. \tag{24}$$

In Eqs. (21)–(24), $1/\tau_1 = K_P P + K_R R$ corresponds to the deexcitation rate of the conduction band ($\tau_1 \approx 8.3 \times 10^{-14}$ s with the constants given here before) and $\tau_2 = (K_P P + K_R R)/K'_R C K_P P$ is the time constant characterizing the evolution of the system towards a thermodynamic quasiequilibrium ($\tau_2 \approx 8.5 \times 10^{-12}$ s).

Assuming, as verified numerically, that $\Delta h/h_0 = \Delta p/p_0 = \Delta c/c_0 = \Delta r/r_0$, the hole modulation is simply given by

$$\Delta h = \begin{cases} msI_0 \tau'_{D_e}\left[1 - \exp\left(-\dfrac{t}{\tau'_{D_e}}\right)\right] & \text{for } t \leqslant \Delta t \\ msI_0 \tau'_{D_e}\left[1 - \exp\left(-\dfrac{\Delta t}{\tau'_{D_e}}\right)\right]\exp\left(-\dfrac{t-\Delta t}{\tau'_{D_e}}\right) & \text{for } t > \Delta t, \end{cases} \tag{25}$$

where $\tau'_{D_e} = \tau_{D_e} h_0/2c_0 = e/\mu'_e k_B T K^2$ is the extrinsic electron diffusion time with $\mu'_e = \mu_e(2c_0)/h_0$ the extrinsic mobility of electrons. For the electron, recombination center, and trap modulation amplitude we get $\Delta c = \Delta h(c_0/h_0)$, $\Delta r = \Delta h(r_0/h_0)$, and $\Delta p = \Delta h(p_0/h_0)$, in accordance with the assumption used to calculate Δh. In order to calculate ΔD and ΔE analytically, we must restrict ourselves to the case when $\Delta t \ll \tau'_{D_e}$, which gives at first order in t/τ'_{D_e}

$$\Delta E = \begin{cases} imE_D\left[1 - \dfrac{t}{2\tau'_{D_e}} - \exp\left(-\dfrac{t^2}{2\Delta t \tau_{di_h}}\right)\right] & \text{for } t \leqslant \Delta t \\ imE_D\left(1 - \dfrac{\Delta t}{2\tau'_{D_e}}\right)\exp\left(-\dfrac{t-\Delta t}{\tau'_{D_e}}\right) & \text{for } t > \Delta t, \end{cases} \tag{26}$$

where $E_D = k_B T K/e$ is the limit space charge field. Examination of Eqs. (25) and (26) for $t > \Delta t$ shows that the measurement of these two quantities allows the determination of τ'_{D_e} or, equivalently, the measurement of the extrinsic electron mobility. Furthermore, measurement of the space charge field during the pulse duration allows the determination of τ_{di_h} or, equivalently, the measurement of the intrinsic hole mobility in $Cd_{1-x}Mn_xTe$.

D. Results for the mean densities

The time evolution of the mean densities c_0, r_0, p_0, and h_0 during the pulse duration are plotted in Figs. 2(a)–2(d) for $\Delta t = 3$ μs and a mean excitation rate corresponding to $sI_0 \Delta t = 10^{16}$ cm^{-3}. In these figures straight and dotted lines correspond to numerical and analytical solutions, respectively. The agreement between numerical and analytical solutions is excellent for all mean densities, the slight misfit observed at long times ($t > 1$ μs) being due to hole recombination, not taken into account in analytical calculations. For much shorter pulse durations [$\Delta t = 100$ ps in Figs. 3(a)–

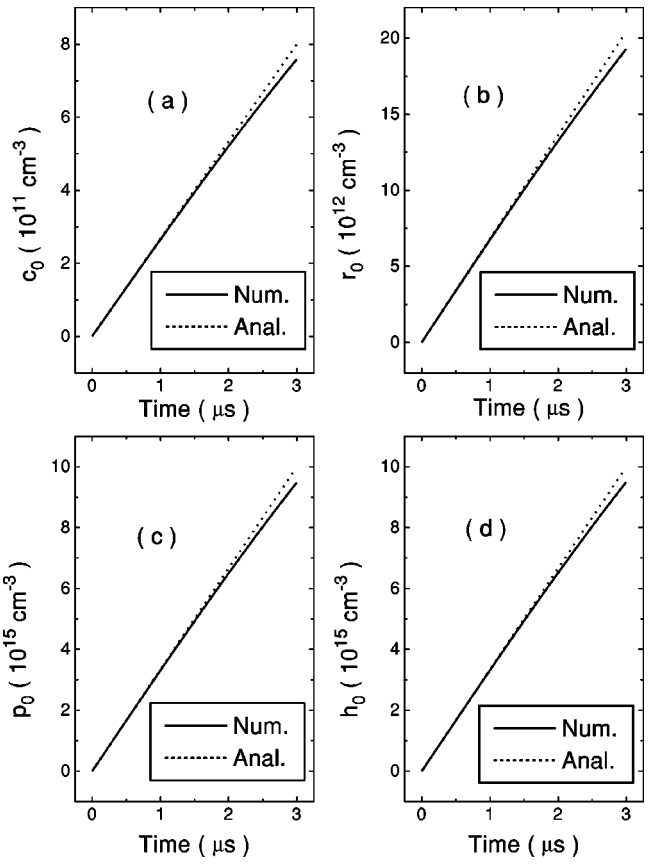

FIG. 2. Temporal evolution of the (a) electron, (b) recombination center, (c) trap, and (d) hole densities during a 3-μs-duration square pump pulse.

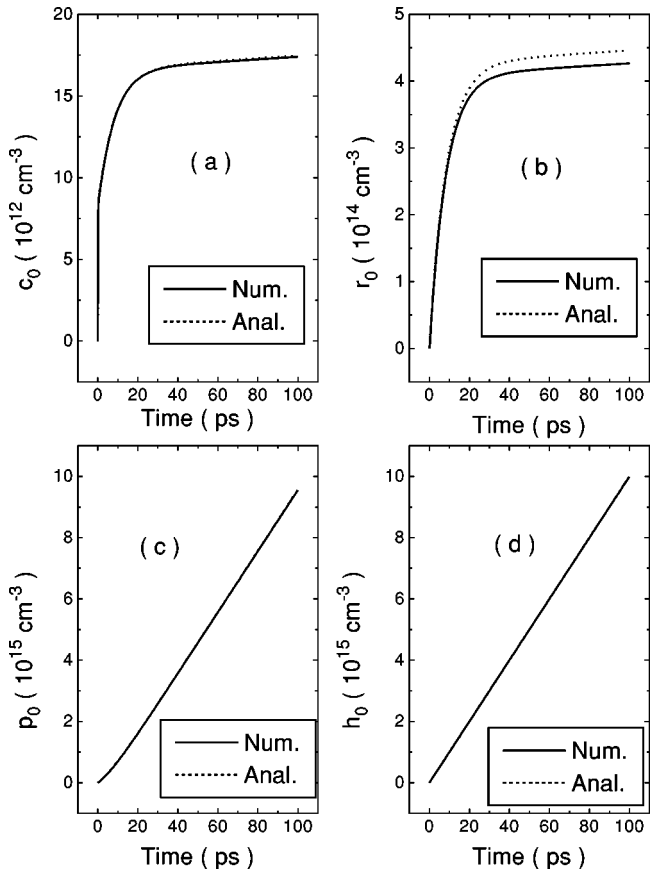

FIG. 3. Temporal evolution of the (a) electron, (b) recombination center, (c) trap, and (d) hole densities during a 100-ps-duration square pump pulse.

3(d)] the agreement is perfect for electrons, holes, and traps and a slight discrepancy exists for the recombination center, which is connected to the high value of r_0 ($r_0 \approx R/20$) reached in such a case. Results presented in Figs. 2 and 3 prove that the analytical solutions describe very well the physical mechanisms over a wide range of pulse durations (typically $\Delta t \approx 100$ ps to 1 μs). For $\Delta t < 100$ ps the approximation $R \gg r_0$ fails badly (at least for our excitation rates) and numerical solutions are required, as for $\Delta t > 1$ μs, when hole recombination must be taken into account.

Examination of Eqs. (21)–(24) shows that for $t \gg 1/K_P'C$ (≈ 2 ns) a quasiequilibrium does exist with $c_0 = h_0 K_P'C/K_P P$, $r_0 = h_0(K_R R K_P'C)/K_P P K_R'C$, and $p_0 = h_0$. Using the numerical values, one gets $c_0/h_0 = 8 \times 10^{-5}$ and $r_0/h_0 = 2 \times 10^{-3}$, in good agreement with the assumption of good trapping of electrons ($p_0/h_0 = 1$). These values are effectively reached for long pulses (see Fig. 2), while for $\Delta t \ll 1/K_P'C$, c_0/h_0 and r_0/h_0 are proportional to $1/\Delta t$ and hence much higher than the equilibrium values (see Fig. 3). However, the quasiequilibrium is reached very rapidly after the end of the laser pulse. This is illustrated in Figs. 4(a)–4(d), which show the numerically calculated time evolution of the mean densities c_0, r_0, p_0, and h_0 for a very short pulse duration ($\Delta t = 10$ ps). A linear scale is used for p_0 and h_0 [Figs. 4(c) and 4(d), respectively], while the use of logarithmic scales in Figs. 4(a) and 4(b) allows the observation of the time evolution of c_0 and r_0, for which the quasiequilibrium ($c_0/h_0 = 8 \times 10^{-5}$ and $r_0/h_0 = 2 \times 10^{-3}$) is reached in a few tens of picoseconds after the high peaks ($c_0/h_0 \approx 0.02$ and $r_0/h_0 \approx 0.2$) obtained during the pulse.

E. Results for the modulation amplitudes

The time evolution of the modulation amplitudes Δc, Δr, Δp, Δh, and ΔE during the pulse duration was calculated both analytically and numerically for a light grating of wavelength $\Lambda = 2.9$ μm having a modulation depth $m = 0.1$. Results presented hereafter were obtained for $\mu_e = 5700$ cm^2/V s and $\mu_h = 40$ cm^2/V s, but they were quite insensitive to the value of μ_h. The value of the intrinsic electron mobility is intentionally a high one in order to validate the approximation $\mu_e c \ll \mu_h h$ of the analytical solution in the most difficult conditions. The calculations performed for pulse durations ranging from 100 ps to 1 μs demonstrate an agreement between analytical and numerical results that is very similar to that obtained for the mean densities (see Figs. 2 and 3). This agreement is indeed consistent with the validity of our assumption of equal relative variations of the populations ($\Delta h/h_0 = \Delta p/p_0 = \Delta r/r_0 = \Delta c/c_0$).

Figures 5(a) and 5(b) show the time evolution of the hole and space charge field modulation amplitudes. These quantities are plotted in Figs. 5(a_1) and 5 (b_1) and Figs. 5 (a_2) and 5(b_2) for pulse durations $\Delta t = 100$ ps and $\Delta t = 10$ ns, respectively. For hole density modulation, the agreement between

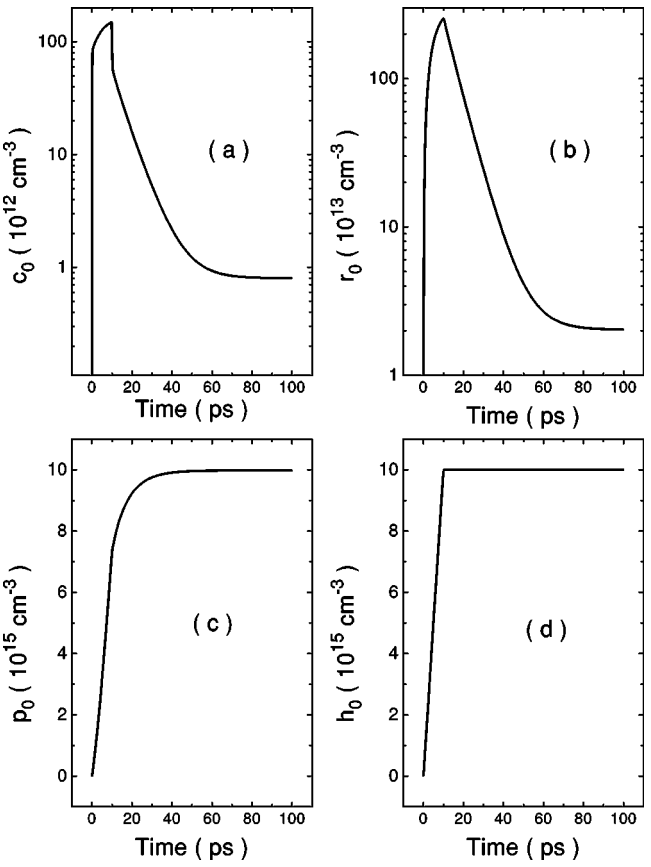

FIG. 4. Temporal recovery of the (a) electron, (b) recombination center, (c) trap, and (d) hole densities after a 10-ps square pump pulse. Electron and recombination center densities are plotted in logarithmic scales.

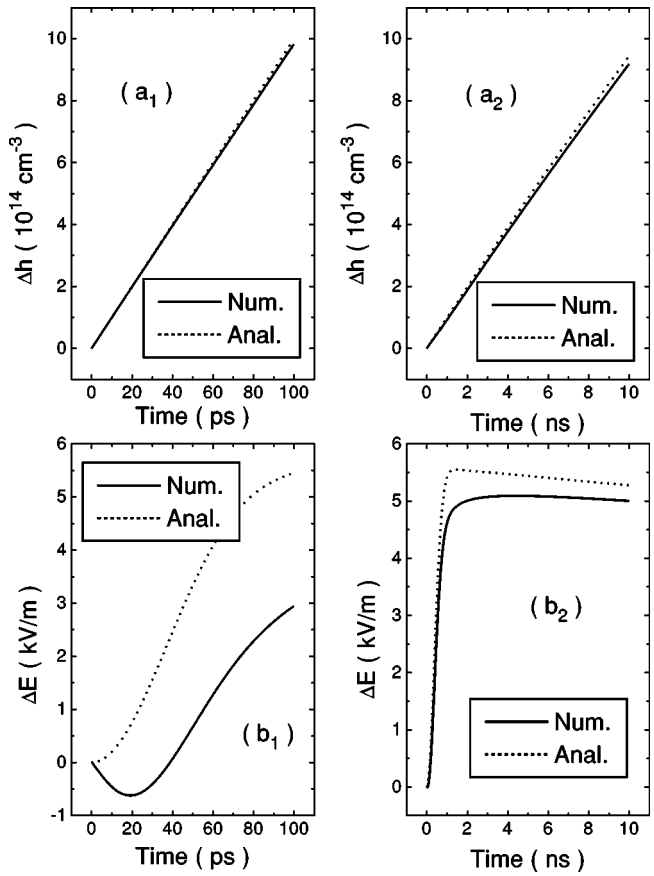

FIG. 5. Temporal evolution of the (a_1) and (a_2) hole and (b_1) and (b_2) space charge field modulations during (a_1) and (b_1) 100-ps and (a_2) and (b_2) 10 ns square write pulses. The light grating modulation depth is $m=0.1$.

numerical and analytical solutions is very good in spite of the numerous approximations, whereas for space charge field modulation, the agreement, which is good for $\Delta t=10$ ns, is rather bad for the shortest pulse duration $\Delta t=100$ ps. This discrepancy is related to the approximation $\mu_e c \ll \mu_h h$, which is no longer valid for a short pulse duration, when c_0 is around 100 times larger than the equilibrium value that is reached in the case of long duration pulses [$\Delta t=10$ ns in Fig. 5(b_2)].

As already mentioned, measurement of carrier mobilities is made possible by examination of the time variation of Δh and ΔE after the laser pulse; Figs. 6(a) and 6(b) show these two quantities plotted on a semilogarithmic scale as a function of time for a pulse duration of 10 ns, which corresponds to that given by our laser. Note that the time scale is very different for the two grating wavelengths used: $\Lambda_1=2.9$ μm [Figs. 6(a_1) and 6(b_1)] and $\Lambda_2=20$ μm [Figs. 6(a_2) and 6(b_2)]. This large difference is due to the diffusion time, which is proportional to the square of the grating wavelength. In the case of the small-wavelength grating [Figs. 5 (a_1) and 5(b_1)] the same exponential decay is calculated numerically and analytically (within few percent) for hole and space charge field modulations; the slope of these straight lines allows the determination of the exponential time constant $\tau'_{D_{e_1}} \approx 87$ ns. In the case of the large-wavelength grating [Figs. 6(a_2) and 6(b_2)] the decay calculated analytically for Δh and ΔE is exponential with the time constant $\tau'_{D_{e_2}} \approx 4.1$ μs [which is related to $\tau'_{D_{e_1}}$ by the relation $\tau'_{D_{e_1}}/\tau'_{D_{e_2}}=(\Lambda_1/\Lambda_2)^2$], whereas the decay calculated numerically is almost exponential [see the continuous straight lines in Figs. 5(a_2) and 5(b_2)], but the time constants are somewhat shorter, due to hole recombination taking place on this time scale. Note that this effect is larger for Δh ($\tau'_{D_{e_2}} \approx 3$ μs) than for ΔD ($\tau'_{D_{e_2}} \approx 3.5$ μs) due to the fact that h_0 is present in both the relaxation and source terms in the differential equation governing the time evolution of Δh while only in the source term in the case of ΔE.

III. EXPERIMENTAL SETUP

The experimental setup used for measurement of carrier mobilities is shown in Fig. 7. It was a classical ''write'' and ''read'' dynamic grating arrangement, similar to that presented in Ref. 7. The grating was recorded by two write beams provided by the same dye laser pumped by a frequency doubled Q-switched Nd:YAG laser (where YAG denotes yttrium aluminum garnet) operating at a 10-Hz repetition rate. The dye laser wavelength was adjusted at $\lambda_W=679$ nm in order to allow a $T=36\%$ transmission of the laser beam through the 3-mm-thick $Cd_{0.7}Mn_{0.3}Te$ sample. The write laser attenuation included 38% of internal losses,

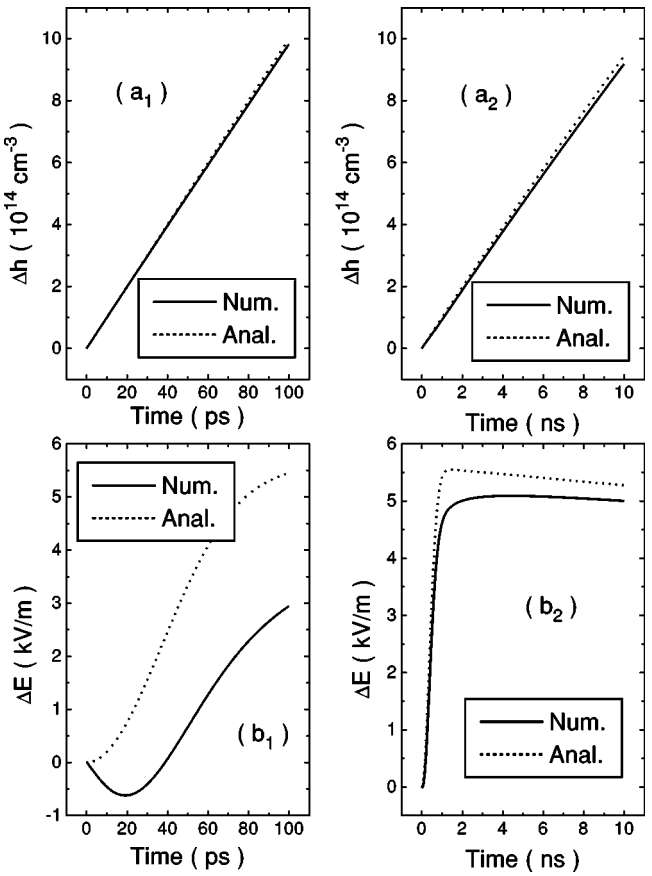

FIG. 6. Temporal relaxation of the (a_1) and (a_2) hole and (b_1) and (b_2) space charge field modulations after a 10-ns square write pulse. (a_1) and (b_1) and (a_2) and (b_2) correspond to 2.9-μm and 20-μm grating wavelengths, respectively. Hole and space charge field modulation are plotted in logarithmic scales in order to show the exponential relaxation.

the remaining losses being due to reflection losses on the uncoated faces of the crystal. Pulse duration was around 10 ns and its fluence on the 3-mm-diam spot was varied up to 3.4 mJ/cm^2 without any optical damage.

The two write beams were sent symmetrically onto the sample at an incidence angle θ_W ranging from 1.1° to 6.7°, which allowed the generation of gratings with a wavelength $\Lambda=\lambda_W/2\sin\theta_W$ ranging from 18 to 2.9 μm. The read beam was delivered by a cw laser diode operating at $\lambda_R=830$ nm and set at the Bragg angle θ_R given by $\sin\theta_R=(\lambda_R/\lambda_W)\sin\theta_W$. Due to the Bragg regime only one strong

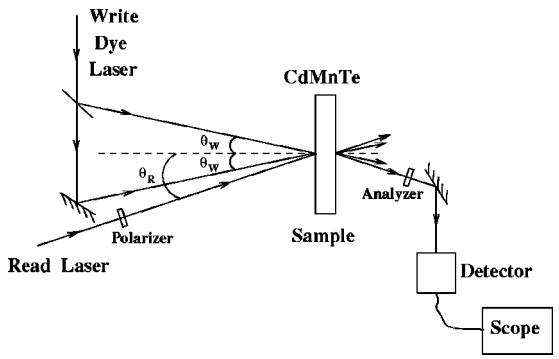

FIG. 7. Experimental setup.

''diffracted'' beam was observed, symmetrically to the transmitted read beam.

Time resolved measurements of the diffracted intensity were ensured by using a fast avalanche photodiode followed by an amplifier. The time-dependent signal was sent to a digital oscilloscope connected to a personal computer in which results were stored and processed. The time resolution of our apparatus was limited to 36 ns due to the strong amplification of the photodiode signal. Polarizers were occasionally added in the paths of the read and diffracted beams in order to obtain a polarization selectivity for the diffracted signal.[8]

IV. EXPERIMENTAL RESULTS AND DISCUSSION

The intensity I_D diffracted by our setup is given by[9]

$$I_D=TI_R\sin^2\left(\frac{\pi\Delta nL}{\lambda_R}\right), \tag{27}$$

where I_R is the read intensity and Δn is the refractive index change induced by the interfering write beams. In our experiment Δn also depends on the polarization directions $\hat{e}_R$ and $\hat{e}_D$ of the read and diffracted beams, respectively, and is given by

$$\Delta n=\hat{e}_D\cdot\Delta\underline{\underline{n}}\cdot\hat{e}_R=\frac{\partial n}{\partial h}(\hat{e}_D\cdot\hat{e}_R)\Delta h-\frac{n_0^3}{2}(\hat{e}_D\cdot\underline{\underline{r}}\cdot\widehat{\Delta E}\cdot\hat{e}_R)\Delta E, \tag{28}$$

where $\partial n/\partial h$ is the derivative of the refractive index with respect to the hole density, $\underline{\underline{r}}$ is the electro-optic tensor, and $\widehat{\Delta E}$ is the unit vector of the space charge field ($\overline{\Delta E}=\Delta E\widehat{\Delta E}$). The contribution due to the hole density $[(\partial n/\partial h)(\hat{e}_D\cdot\hat{e}_R)\Delta h]$ is in fact about 10 times larger than that related to the space charge field;[8] it can therefore be measured alone (within 1% precision) without any polarizer. The space charge field contribution was measured with a diffracted polarization orthogonal to the read one, which eliminates the strong hole contribution. In order to simplify the fitting procedure and therefore gain reliability, the experiment was performed at relatively low excitation so that I_D was proportional to Δh^2 without any polarizer and to ΔE^2 for crossed read and diffracted polarizations. Due to the low excitation level, we had to use write pulses with the same energy ($m=1$), which allowed us to follow the diffracted intensity over a sufficiently long time for a precise measurement of the time constants. This situation did not correspond to the perturbative solution of the population dynamics presented in Sec. II B. However, under our approximation of equal relative densities ($\Delta h/h_0=\Delta p/p_0=\Delta r/r_0=\Delta c/c_0$), we immediately see from Eq. (18) that the time evolution of the hole density modulation is linear in Δh and m, so that only the first order can exist in the Fourier development of Δh. The perturbative solution for hole modulation amplitude is therefore also valid for $m\approx1$. This is not the case for the space charge field modulation, given by a differential equation that is nonlinear with respect to populations [see Eq. (19)]. A more refined calculation is then required following, for instance, the procedure of Ref. 10 used in the case of photorefractive materials.

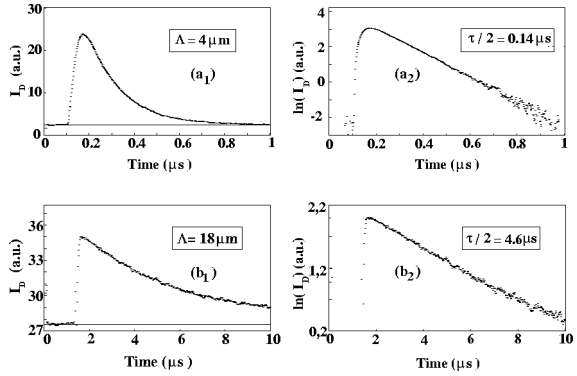

FIG. 8. Diffracted signals plotted in (a_1) and (b_1) linear and (a_2) and (b_2) logarithmic scales obtained with (a_1) and (a_2) $\Lambda = 4\ \mu$m and (b_1) and (b_2) $\Lambda = 18\ \mu$m. $\tau/2$ is the relaxation time of the diffracted intensity.

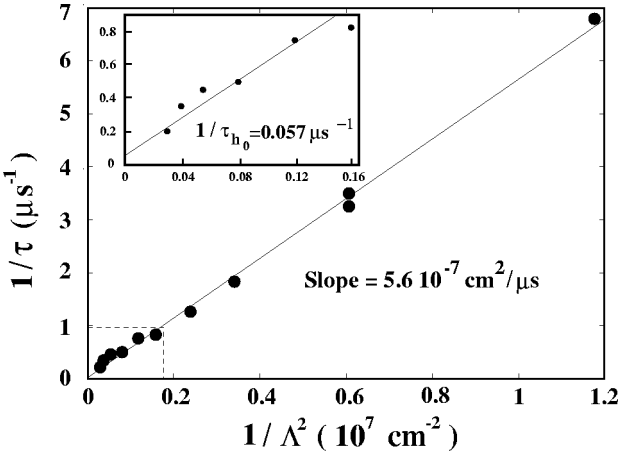

FIG. 9. Relaxation rate of the optically encoded diffraction gratings as a function of the squared grating frequency. The inset shows a magnification of the curve for small Λ^{-2} in order to determine the electron-hole recombination time.

The time evolution of the total diffracted intensity (without polarizer) was measured for different values of the grating wavelengths. Figures 8(a_1) and 8(a_2) and Figs. 8 (b_1) and 8(b_2) show results obtained for $\Lambda = 4$ and 18 μm, respectively. The measured signals and their natural logarithms are plotted in Figs. 8(a_1) and 8(b_1) and Figs. 8(a_2) and 8 (b_2), respectively. As seen from Figs. 8(a_1) and 8(b_2), the decay is exponential over a wide range [four and two time constants in Figs. 8(a_2) and 8(b_2), respectively], thus providing precise measurements of the relaxation times. Figure 9 shows the inverse relaxation times of the index grating $1/\tau$ plotted as a function of Λ^{-2}. Although hole recombination is not exponential in our model [see Eq. (9)], we consider it exponential for a very short time, right at its beginning, which is always possible. This approximation enables us to write $1/\tau$ as a sum of a recombination term and a diffusion term

$$\frac{1}{\tau} = \frac{1}{\tau_{h_0}} + \frac{1}{\tau_{D_e'}} = \frac{1}{\tau_{h_0}} + \frac{\mu_a k_B T K^2}{e}. \tag{29}$$

From the slope a of the experimental curve, we deduce the ambipolar mobility in our sample $\mu_a = 0.54$ cm^2/V s. As this value is much smaller than the intrinsic hole mobility, we have $\mu_a \approx \mu_e'$, which corresponds to an intrinsic mobility $\mu_e = \mu_e' h_0 / 2c_0 = 3375$ cm^2/V s, a value that is somewhat higher than that measured in CdTe ($\mu_e = 1100$ cm^2/V s).[1]

A fit of the relaxation rate around $K \approx 0$ (see the inset of Fig. 9) allows the determination of the hole lifetime ($\tau_{h_0} = 18\ \mu$s) with a precision of around 20%, provided we used for μ_e' the value determined for large wave vectors. This value of τ_{h_0} is in good agreement with the initial hole lifetime calculated numerically with no adjustable parameters ($\tau_{h_0}' = 20\ \mu$s).

Concerning the time evolution of the space charge field, experiments were performed with crossed diffracted and read polarizations, although the corresponding results cannot be directly compared with those obtained theoretically with the high contrast value ($m \approx 1$) of the light grating. Unfortunately, the signal to noise ratio obtained in these experiments was not good enough to provide exploitable results. A higher read laser power and/or a longer crystal would be necessary for this purpose, especially if a direct comparison with theoretical results is wanted.

V. CONCLUSION

Carrier diffusion in $Cd_{1-x}Mn_xTe$ has been investigated both theoretically and experimentally by the grating technique. Due to the efficient trapping of electrons, most probably on manganese sites, the effective electron mobilities is strongly reduced as well as electron-hole recombination. Moreover, generation of a space charge field of the order of several kV/m was predicted. A simple analytical solution to the coupled differential equations expressing population dynamics, charge continuity, and Poisson's law was found to be in excellent agreement with numerical calculations for a large range of durations of the write pulses (from 100 ps to 1 μs). Using published values of the relaxation constants, a reduction of electron mobility by a factor of 6000 was calculated. Calculations were compared with experimental results obtained by reading, with a cw laser diode, gratings encoded in the SMSC's by two interfering nanosecond laser pulses. From the measurement of the time evolution of the diffracted signal for different grating wavelengths, a recombination lifetime of 18 μs was measured and found to be in good agreement with the calculated value (20 μs); an ambipolar mobility of 0.54 cm^2/V s was also measured, which corresponds to an intrinsic mobility of about 3400 cm^2/V s for free electrons in $Cd_{0.7}Mn_{0.3}Te$. This value is somewhat higher than that measured in CdTe [1100 cm^2/V s (Ref. 1)]. The ambipolar mobility obtained in $Cd_{0.7}Mn_{0.3}Te$ is therefore about 100 times smaller than in pure CdTe, which could make this efficient material[8] potentially interesting for parallel optical information processing in the microsecond range.

ACKNOWLEDGMENT

The authors acknowledge Dr. R. Triboulet for providing the high-quality $Cd_{1-x}Mn_xTe$ sample used in the experiments.

[1] B. Segall, M. R. Lorentz, and R. E. Halsted, Phys. Rev. **129**, 2471 (1963).

[2] R. Pankoke, C. Buss, S. Hugonnard-Bruyère, P. Leisching, R. Frey, and C. Flytzanis, Appl. Phys. Lett. **68**, 2615 (1996).

[3] See, for example, H. J. Eichler, P. Gunter, and D. W Pohl, in *Laser-Induced Dynamical Gratings*, edited by H. J. Eichler, P. Gunter, and D. W. Pohl, Springer Series in Optical Science Vol. 50 (Springer, Heidelberg, 1987); R. K. Jain and M. B. Klein, *Optical Phase Conjugation* (Academic Press, New York, 1983), p. 307.

[4] S. Hugonnard-Bruyère, Ph.D. thesis, Ecole Polytechnique, Palaiseau, 1994.

[5] S. Hugonnard-Bruyère, C. Buss, R. Frey, and C. Flytzanis, Appl. Phys. Lett. **66**, 2043 (1995).

[6] R. Wojtal, A. Golnik, and J. A. Gaj, Phys. Status Solidi B **92**, 241 (1979).

[7] A. Vanhaudenarde, M. Trespidi, and R. Frey, J. Opt. Soc. Am. B **11**, 1474 (1994).

[8] C. Moussu, I. Zaquine, A. Maruani, and R. Frey, J. Cryst. Growth **184/185**, 701 (1998).

[9] H. Kogelnik, Bell Syst. Tech. J. **48**, 2909 (1969).

[10] N. V. Kukhtarev, P. Buchhave, and S. F. Lyuksyutov, Phys. Rev. A **55**, 3133 (1997).